Nanoscale

Accepted Manuscript

This article can be cited before page numbers have been issued, to do this please use: H. Zhang, S. Chen, H. Xia and K. Wang , *Nanoscale*, 2026, DOI: 10.1039/D5NR05504K.

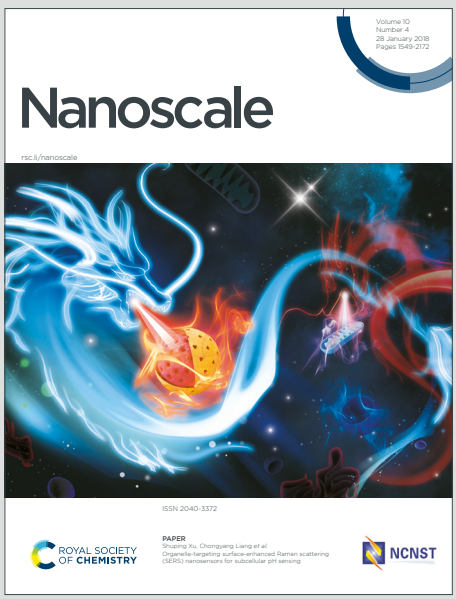

ROYAL SOCIETY OF CHEMISTRY

rsc.li/nanoscale

View Article Online
DOI: 10.1039/D5NR05504K

Carbolong Complexes: An Emerging Class of Metallaaromatics for Next-Generation Functional Materials

Haixin Zhang[1], Shiyan Chen[2]*, Haiping Xia[2], Kun Wang[1,3]*

1. Department of Physics, University of Miami, Coral Gables, Florida 33146, USA
2. Shenzhen Grubbs Institute and Guangdong Provincial Key Laboratory of Catalysis, Department of Chemistry, Southern University of Science and Technology, Shenzhen 518055, China.
3. Department of Chemistry, University of Miami, Coral Gables, Florida 33146, USA

* Corresponding Author: kunwang@miami.edu (K. W.), chensy6@sustech.edu.cn (S. C.)

Abstract

Aromaticity and antiaromaticity represent fundamental pillars of chemical stability, reactivity, and performance. As a distinctive aromatic complex with metallaaromaticity, carbolong complexes featuring metal-carbon conjugated polycyclic metallacycles have emerged as an intriguing class of compounds in organometallic chemistry, biomedical science, and material sciences. Characterized by a long carbon chain chelated to a metal center via multiple metal-carbon bonds, these complexes exhibit rare Craig aromaticity in addition to Hückel topologies. This unique electronic structure confers exceptional stability, extensive electron delocalization, and highly tunable optoelectronic properties. This review provides a comprehensive analysis of the synthetic strategies and design principles governing carbolong chemistry. We highlight recent advances in single-molecule charge transport of carbolong molecules, integration of carbolong complexes into high-efficiency solar cells, and their burgeoning potential in photothermal therapy and molecular optoelectronics. By bridging the gap between fundamental metallaaromaticity and functional materials science, this work serves as a strategic roadmap for researchers leveraging carbolong chemistry and related design principles to drive the development of next-generation optoelectronics, energy conversion, and biomedical technologies.

View Article Online
DOI: 10.1039/D5NR05504K

1. Introduction

Aromatic compounds, with cyclic delocalized π conjugation, construct one of the most fundamental chemical families.[1–5] Due to their enhanced stability compared to other saturated compounds, organic aromatics have been widely used in chemical synthesis,[6,7] materials engineering,[8–10] biochemistry,[11–13] nanotechnology,[14] and industry.[15–17] In addition, antiaromatic compounds with similar cyclic structures but different numbers of delocalized π electrons exhibit narrower HOMO-LUMO gap and efficient charge transport,[18–20] offering new opportunities in organic semiconductors,[21,22] nanoelectronics,[23,24] and energy storage materials.[25,26] Therefore, aromaticity and antiaromaticity constitute the conceptual basis for structure–property relationships in π-systems, governing stability, reactivity, and electronic response across organic and organometallic chemistry.

As a unique kind of aromatic compounds, metallaaromatics include one or more metal atoms in the aromatic cycle(s).[27–29] Metallabenzene, the first, simplest, and most researched metallaaromatic compound, was theoretically predicted by Thorn and Hoffman[30] and synthesized and characterized by Roper et al.[31] in the 1900s. Over the past few decades, besides metallabenzenes,[32,33] a variety of metallaaromatics have been synthesized and investigated, including metallabenzynes,[34–37] heterometallaaromatics,[38–42] spiro metalloles,[43] dianion metalloles,[44–46] metallapentalenes,[47,48] and metallapentalynes.[48–50] Differential from conventional molecules only containing pπ-pπ conjugation, embedded metal atoms in metallaaromatics provide dπ electrons conjugated with carbon atoms, creating dπ-pπ conjugation, which uniquely combine the properties of organic aromatics and organometallics.[28,51–53] This dπ-pπ conjugation modulates molecular orbital profiles and consequently optical absorption and charge transport behaviors.[48,54] These exceptional properties provide broad and substantial applications in solar cells,[55,56] memory materials,[57,58] optoelectronics,[59,60] and phototherapy materials.[61,62] Furthermore, compared with traditional organometallics, the metal-engaged aromatic ring effectively enhances stability due to aromaticity.[2,63–65] Therefore, in catalytic chemistry, metallaaromatics, especially multi-metal-atoms metallaaromatics with synergism between the multiple metal centers, often exhibit superior catalytic performance.[66,67]

Metal-carbon bonds, as the most fundamental features of organometallic chemistry, have been broadly applied in various fields, including material science,[68,69] applied physics,[70,71] biology,[72–74] and industrial engineering.[75–77] However, polydentate metal-carbon chelation is rare since most metals prefer to chelate with heteroatoms as lower energy rather than with carbon atoms.[48] In 2013, Xia's group synthesized a planar metallapentalyne that belongs to the class of Craig-type aromatic systems,[49,78] thereby demonstrating aromatic stabilization in a [4n] π-electron framework, in contrast to the classical Hückel[79] [4n+2] aromatic rule.[80,81] This molecule has three metal-carbon bonds as a 7-carbon (7C) chain coordinated with a metal atom in the center, forming tridentate chelation. A series of novel polycyclic frameworks were recently created with an extended carbon chain from 7C to 12C or even 15C.[48] Notably, the 15C complex represents the first metal-centered [15]annulene. Today, the planar conjugation systems of the long unsaturated carbon chain (not less than 7C) coordinated to a transition metal atom with at least three metal-carbon bonds are termed carbolong chemistry.[82,83] Due to the unique dπ-pπ conjugation from the embedded metal

View Article Online
DOI: 10.1039/D5NR05504K

atom, carbolong complexes yield outstanding chemical and physical features, such as chemical and structural stability,[49] high electron transmission,[84] broad light absorption,[85] and stable photothermal effect.[86] These special properties hold promise for expanding the application of carbolong chemistry in nanoelectronics,[59,87] synthetic chemistry,[88] material science,[89] and biomedicine.[90–92]

To highlight the development of and stimulate interest in emerging carbolong complexes for emerging functional applications, this review survey recent advances in both synthesis and applications of carbolong chemistry, with a special focus on nanoelectronics, energy conversion, and optoelectronics (**Figure 1**). The synthesis and design sections delve into the synthetic strategies employed, highlighting key achievements, and tunable modification of carbolong complexes. The carbolong electronics section focuses on recent advancements in single-molecule charge transport investigations and applications in solar cells, providing insights into the electronic properties of carbolong complexes. Furthermore, the photoresponsive application section explores the application in photothermal devices and the potential of employing carbolong chemistry in optoelectronics and thermoelectric molecular devices.

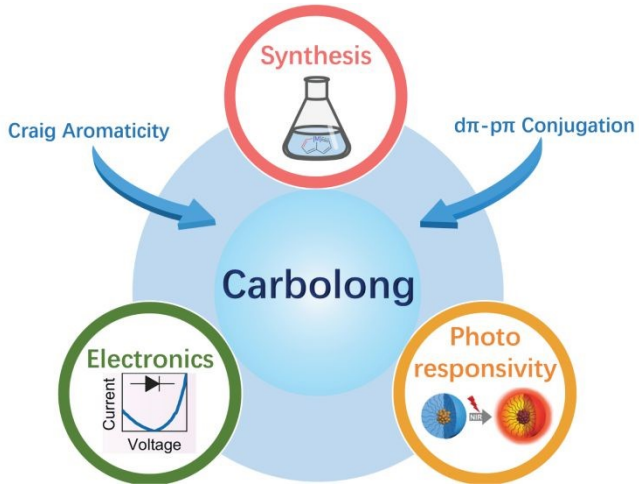

Figure 1. Scheme of the structure of this review.

2. Design and Synthesis of Carbolong Complexes

From the first discovery of benzene by Michael Faraday in 1825,[93] aromaticity has a history of around 200 years. As one of the most fundamental chemical concepts and properties, it depicts the special stability of some cyclic compounds, for example, benzene and its derivatives,[94] annulenes,[95] heteroaromatics,[96] and fullerenes.[97] Although aromaticity is an inherent property of molecules, it contains some typical characteristics,[28,81,98–100] such as planarity, Hückel rule, bond length equalization, deshielding of exocyclic protons in the ^{1}H NMR spectrum, and so on. In planar cyclic compounds, Hückel's rule explains that [4n+2] delocalized π-electron structure in the ring indicates aromaticity, while antiaromaticity with [4n] π electrons. However, carbolong complexes, by replacing one of the bridgehead carbons with a transition-metal atom, change the

View Article Online
DOI: 10.1039/D5NR05504K

antiaromaticity of parent organic analogues to Craig-type aromaticity. The inserted *d* orbital from the metal atom into the conjugation ring system renders Craig aromaticity with the opposite electron rule: the compound has aromaticity with [4n] delocalized π electrons and antiaromaticity with [4n+2] π electrons. For example, pentalyne as the parent organic compound of metallapentalyne is Hückel antiaromatic, but metallapentalyne shows a Craig aromaticity.[49] Therefore, carbolong complexes exhibit stability attributed to intrinsic aromaticity.

There are two major synthesis strategies for constructing carbolong frameworks. One is step-by-step synthesis, in which the skeleton carbon atoms increase by adding alkynes stepwisely.[48] As a result, the carbon chain coordinated with metal atoms in the center can be extended from 7C to 12C or even 15C. However, the metal variety can only be osmium (Os) in this synthesis method. The other is one-pot approach, which uses multiyne chains chelating metals.[101] Besides the simple and convenient procedures, the metal variety can extend to osmium, ruthenium, rhodium, and iridium. In this section, these two synthesis strategies will be elaborated in detail.

2.1 Step-by-step synthesis of carbolong frameworks

According to the different number of chelated carbon atoms in the carbolong skeleton, it could be designated as 7C carbolong complex, 8C carbolong complex, and so on (**Scheme 1**). The additional carbon atoms source can be alkynes or isonitriles.

Scheme 1

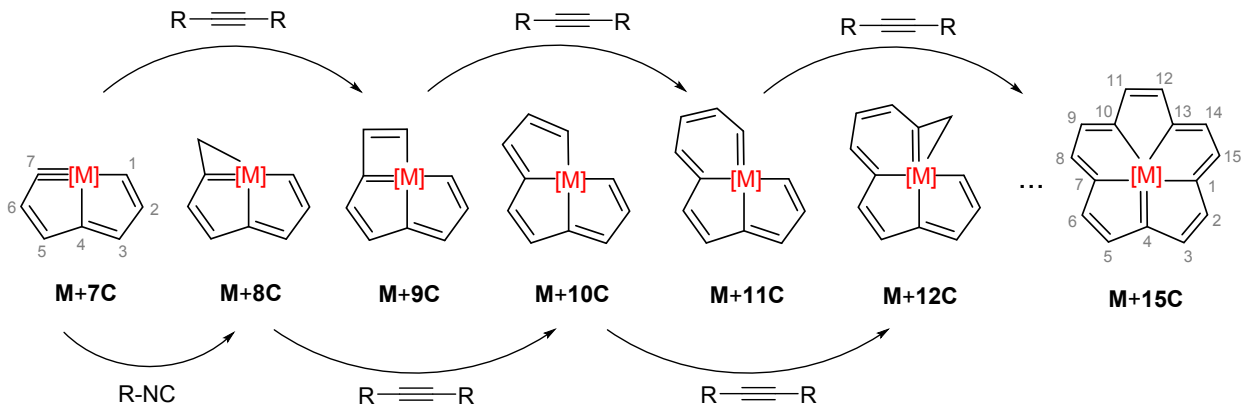

In 2013, Xia and Zhu et al. reported the synthesis of metallapentalyne (7C carbolong complex).[49] Treatment of osmium precursor complex **S1** with methyl propiolate in dichloromethane at room temperature (RT) could obtain the 7C carbolong complex **1** in high isolated yield. It is worth noting that it contains a carbyne bond with the M≡C–C angle of ~130° in an extremely strained structure. The inherent Craig aromaticity could overcome its high ring strain, which may account for the stability of **1**. After adding acid, there was a tautomeric shift of the metal-carbon triple bond from the initial ring to a different five-membered ring.[102]

View Article Online
DOI: 10.1039/D5NR05504K

Scheme 2

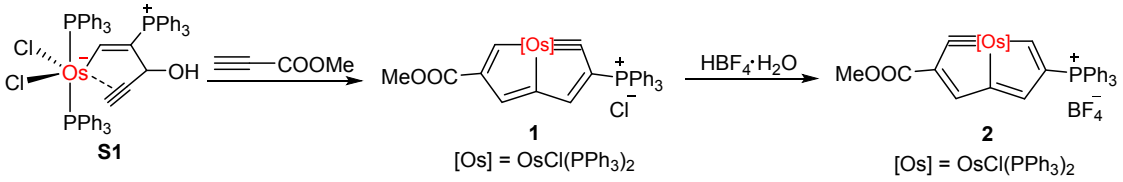

The metal-carbon triple bond of metallapentalyne **1** can be reacted with quantitative isocyanides through [2+1] cycloaddition, which directs the formation of η^2-iminoketenyl complexes **3** (8C carbolong framework).[103] This species has been postulated as the intermediates in nucleophile-induced carbyne–isocyanide C–C coupling processes. A similar 8C carbolong framework **4** could also be obtained by Treatment of osmium precursor complex **S1** with allenylboronic acid pinacol ester.[104] There is σ-aromaticity in the unsaturated three-membered ring, which is supported by experimental observations and theoretical calculations.

Scheme 3

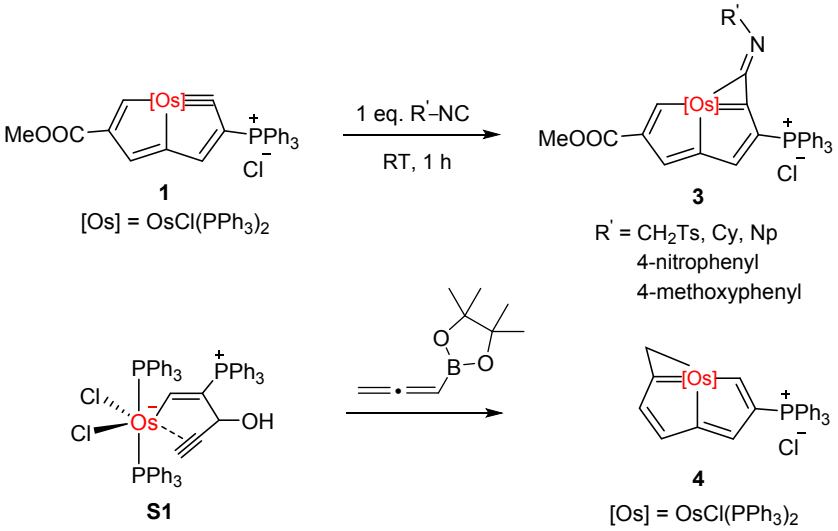

The 9C carbolong framework **5** could be constructed by the [2+2] cycloaddition of metallapentalynes and alkynes.[105] Cyclobutadiene and pentalene are antiaromatic species, which are substantially less thermodynamically stable than aromatic moieties. However, using one transition metal could stabilize these two antiaromatic frameworks simultaneously, reflected by the good stability of carbolong complexes **5**. Interestingly, metallacyclobutadiene **6** could be converted to metallacyclopropene **7** upon adding trifluoroacetic acid. The realization of photoresponsivity structurally defined ring contraction was driven by π- and σ-aromaticity relays.[106]

View Article Online
DOI: 10.1039/D5NR05504K

Scheme 4

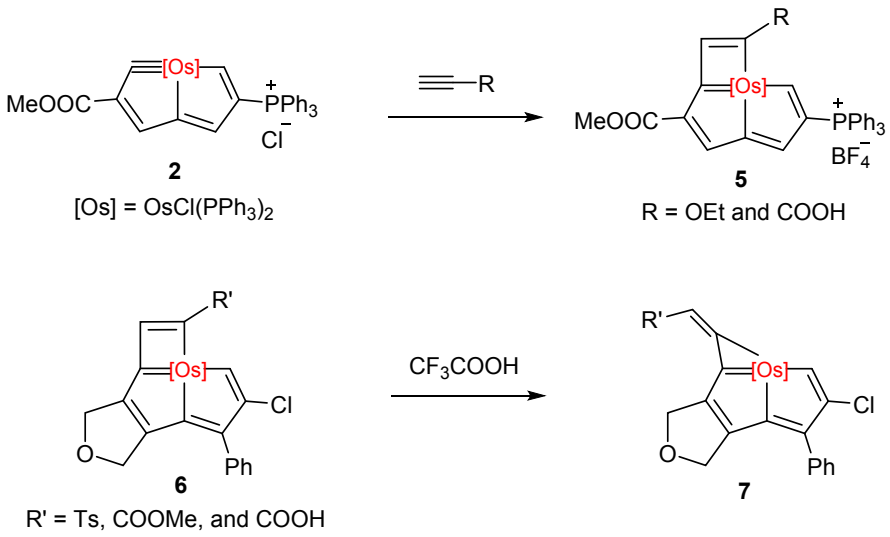

Unsaturated metallacyclopropenes were usually regarded as "three-atom synthons" with high reactivities, which could undergo [3+2] cycloaddition with various unsaturated substrates.[107] The chlorine ligand of complex **4** would be left with the treatment of silver tetrafluoroborate. Subsequently, the strained three-membered ring of osmapentalenes undergoes [3+2] cycloaddition with alkynones, leading to a 10C carbolong framework **8**. The three fused five-membered rings were both aromatic. However, they were non-aromatic in *t*-BuNC substituted complex **9**.

Scheme 5

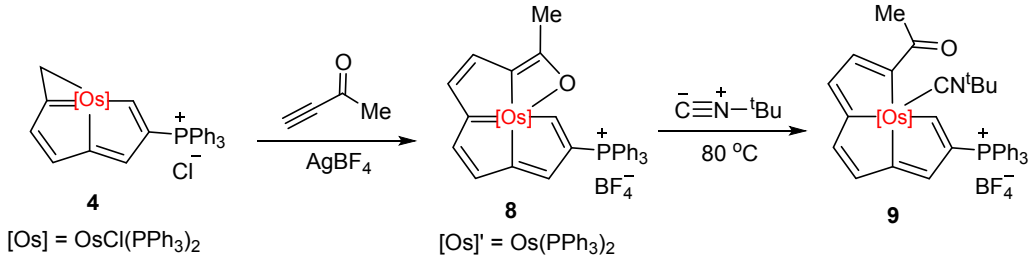

The 11C carbolong framework **11** could be obtained by the [2+2+2] cycloaddition of metallapentalynes and alkynes.[108] The [2+2] cycloaddition intermediate **A** was first formed with the insertion of an alkyne. Then, intermediate **A** could react with another molecule of alkyne to generate an 11C carbolong framework. The resulting osmium six-membered ring structure does not have a stable planar spatial configuration. It could be converted to a more thermodynamically stable complex **12** under heating conditions.

View Article Online
DOI: 10.1039/D5NR05504K

Scheme 6

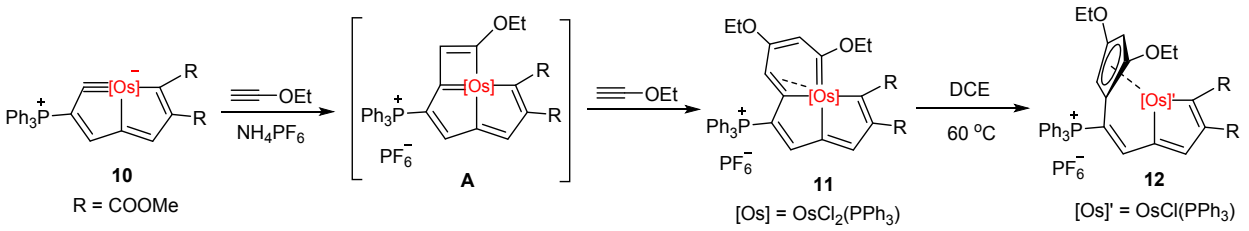

Using the carbon chain-growing strategy, the 12C carbolong framework **13** and **14** could be easily constructed by adding alkynes or allenylboronic acid pinacol ester to the 8C carbolong framework **4** in the presence of $AgBF_4$.[92] This type of osmium complex represents the highest number of coordinated carbon atoms in the equatorial plane. The large π-conjugation with good aromaticity exhibits broad and strong ultraviolet-visible-near-infrared absorption bands and excellent photothermal properties.

Scheme 7

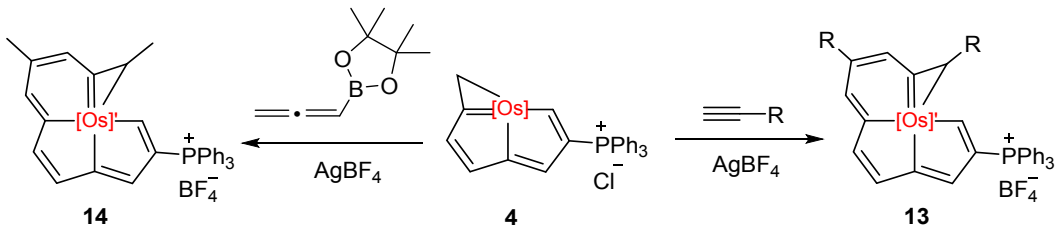

The 15C carbolong framework **20** consists of five fused five-membered aromatic rings and exhibits overall D_{5h} symmetry (**Scheme 8**).[109] These compounds were synthesized from 11C carbolong complexes.[110–112] Alkynyl-substituted complexes **16** were obtained by treating complex **15** with alkynyl lithium reagents. Subsequently, complex **16** underwent a cycloaddition reaction with TsC≡CH to afford the metal-centered [15]annulene **17**. Interestingly, a series of skeleton transformations based on the 15C carbolong framework were observed under different reaction conditions. Ultimately, a molecule with a "Chinese plum blossom"–like architecture was successfully synthesized.

View Article Online
DOI: 10.1039/D5NR05504K

Scheme 8

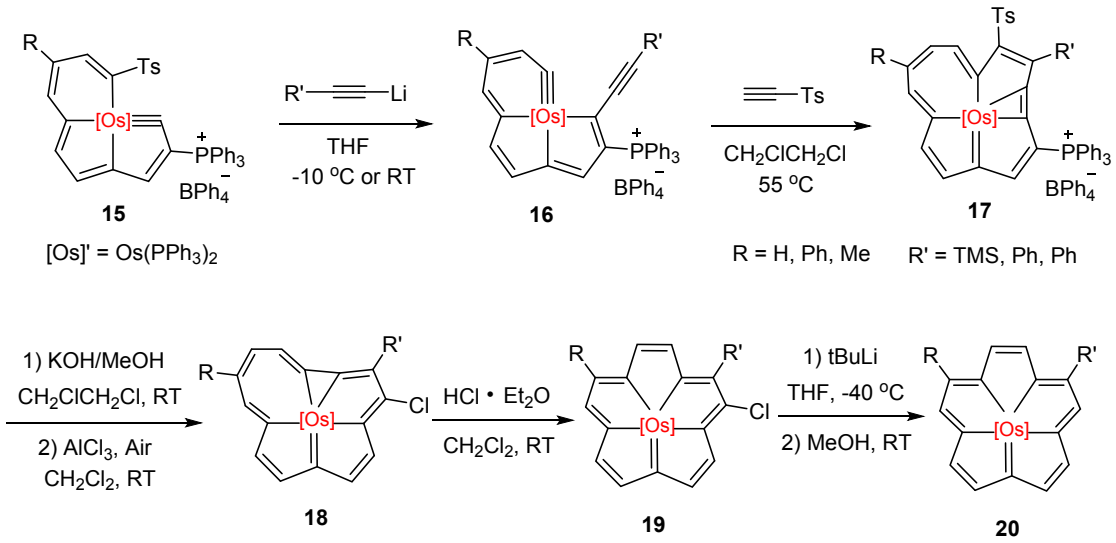

2.2 One-pot synthesis of carbolong frameworks

Chelating transition metals with multiyne chains could generate carbolong frameworks in a one-pot synthesis.[101] The direct reactions of these multiyne chains with commercially available substrates (complexes of osmium, ruthenium, rhodium, and iridium), even simple metal salts, afford an atom-economic, convenient, and efficient one-pot strategy for constructing tridentate carbon-ligated chelates under ambient conditions on gram scales. The core structure of multiyne chains ligand consists of three parts: 1,4-pentane-3-ol, flexible alkyl linking groups, and terminal alkynes.

Scheme 9

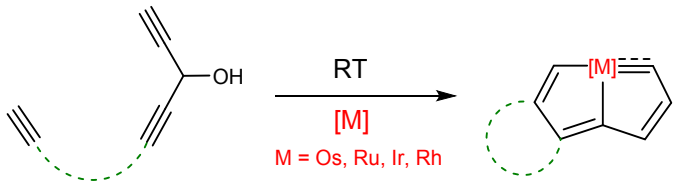

As shown in **Scheme 10**, in the structure of multiyne **L1**, three C≡C triple bonds are separated by sp^3-hybridized carbon atoms. Specifically, the three consecutive sp^3 carbon atoms were designed to form a five-membered carbocycle with the other two *sp* carbon atoms, which may facilitate the binding of the carbons to the metal center. The readily feasible combination of multiyne chain **L1** with metals gives rise to a versatile carbon-chelating platform that can produce carbolong frameworks with four different metal centers (Osmium, Ruthenium, Iridium, and Rhodium).[101,110,113,114] In short, multiyne chains act as a carbon scarf to access chelates with three metal-carbon bonds.

View Article Online
DOI: 10.1039/D5NR05504K

Scheme 10

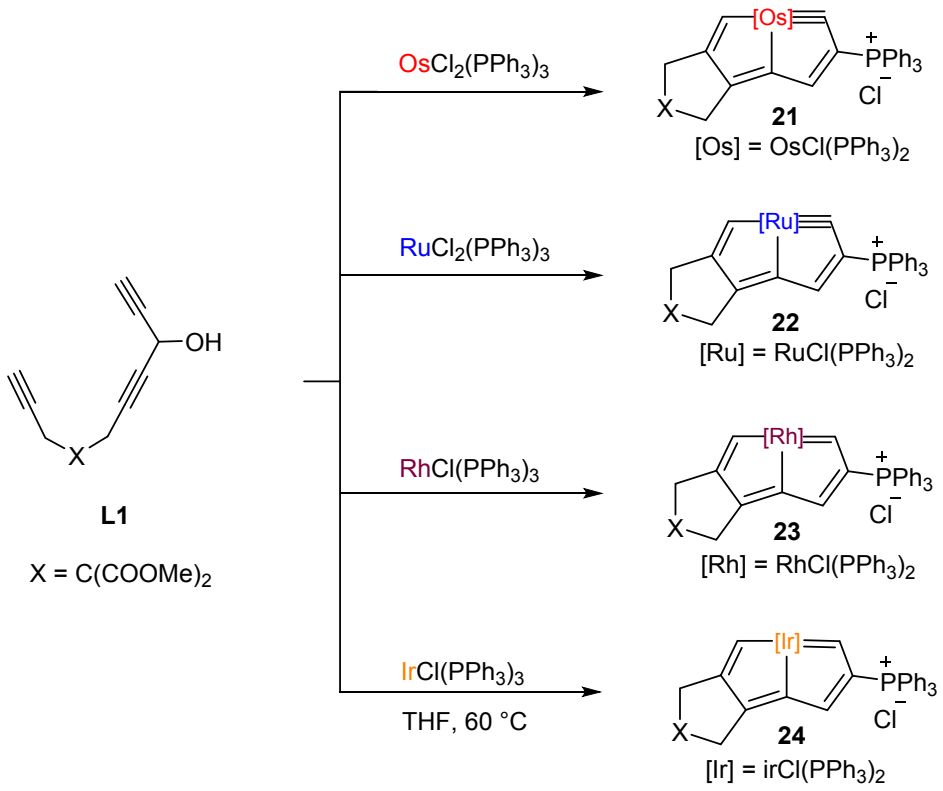

By modifying the terminal alkynes of the multiyne chains with 1,3-butyldyne (**L2**), dienyl (**L3**), and ortho phenol (**L4**) substituents, different carbolong derivatives (**25**, **26**, and **27**) could be easily generated, respectively.[101] Specifically, during the conversion process of compounds **L2** to **26**, all eight *sp* hybridized carbon atoms and 1 sp^3 hybridized carbon atom were converted into sp^2 hybridized carbons, demonstrating the strong chelating ability of the multiyne chains ligand. In a word, the multiyne chains exhibit strong chelating ability reflected by the one-pot strategy via multiyne chains chelating transition metals, providing a facile, efficient methodology for preparing carbolong frameworks.[52,115,116]

View Article Online
DOI: 10.1039/D5NR05504K

Scheme 11

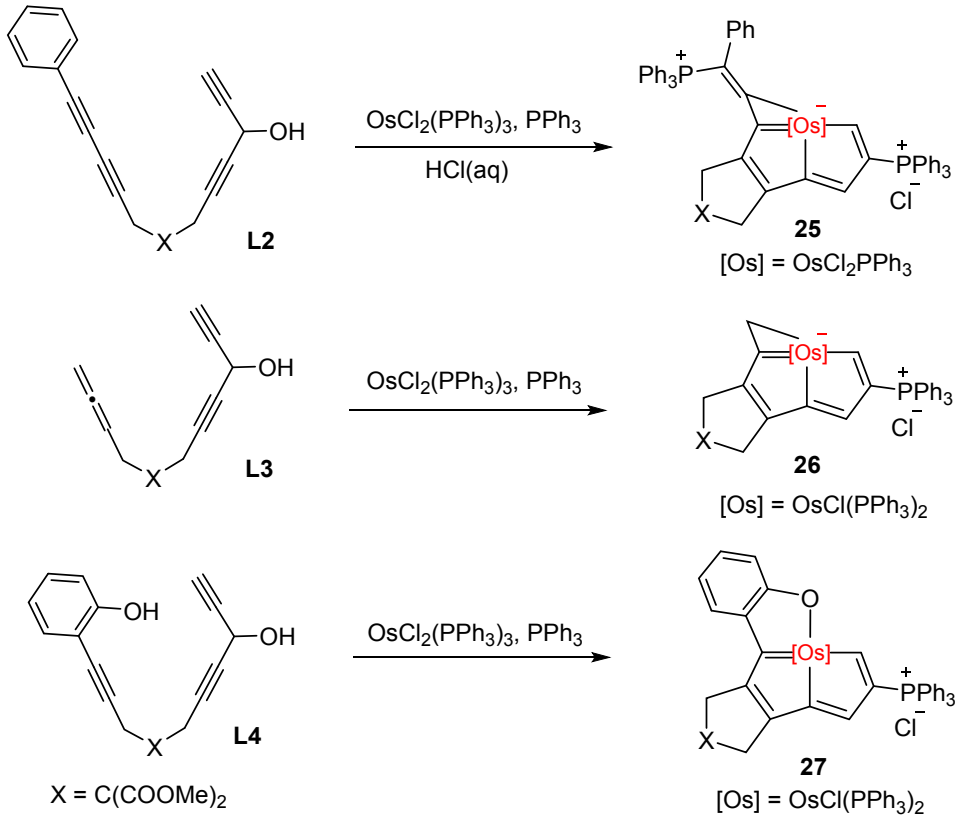

2.3 Fundamental properties relevant to applications

Carbolong frameworks arise when a conjugated carbon chain chelates a transition metal through multiple independent M–C bonds. The resulting metallacycles display Craig-type aromaticity in [4n] π systems and retain planarity through polydentate carbon coordination. These structural features stabilize unusually high carbon coordination at the metal center and create a rigid, delocalized pathway across the metal–carbon scaffold, which is essential for reproducible transport and processing stability.[83]

The electronic structure couples metal d orbitals with the π manifold and compresses the optical gap. As a result, carbolong complexes commonly show strong and broad absorption that extends from the ultraviolet to the near-infrared (NIR) region. The absorbed energy can relax radiatively or dissipate as heat or ultrasound, giving photoluminescence together with efficient photothermal and photoacoustic responses.[52]

Charge-transport and interfacial characteristics connect these molecular traits to device performance. Carbolong motifs function as electron-transmission building blocks and as interlayers in photovoltaic devices. Their interfacial dipoles can downshift electrode work functions and promote charge extraction, which supports both efficiency and operational stability.[117] The same chelating design can be embedded in polymer backbones to deliver processable films that retain the underlying electronic features. These properties provide a direct

View Article Online
DOI: 10.1039/D5NR05504K

bridge from molecular architecture to the transport, optical, and interfacial functions discussed in the following application sections.[83]

3. Optoelectronic Applications of Carbolong Complexes

Efficient charge transport and robust chemical stability represent two fundamental prerequisites in the design and development of advanced optoelectronic devices. As an emerging class of metallaaromatics, carbolong complexes, by virtue of their extended π-conjugation and high aromaticity, exhibit both excellent charge transport characteristics and exceptional chemical stability. This combination of properties, coupled with their tunable charge transport behavior, render them promising for applications in next-generation nanoelectronics, including sensors, molecular switches, and diodes.[118–120] Consequently, the application-driven synthesis of functional metallaaromatics is significantly expanding the horizon of advanced functional electronics and sustainable energy technologies, such as solar cells.[54] The unique charge transport properties of carbolong complexes, stemming from the dπ-pπ conjugation inherent in their multiple metal-carbon bonds and polydentate chelation, are particularly favorable for their integration into single-molecule electronics,[59,87] organic solar cells (OSCs),[55,121] and perovskite solar cells (PSCs).[56,122,123] Furthermore, the enhanced stability conferred by the complexes' aromaticity often leads to a longer operational lifetime and sustained high efficiency in solar cell devices.[54] This section will delve into the distinct advantages and current applications of carbolong complexes within the fields of molecular electronics and photovoltaic devices.

3.1 Carbolong-based single-molecule electronics

Device scaling is approaching fundamental limits from quantum tunneling and power dissipation, pushing conventional solid-state materials toward the bounds of Moore's Law.[124] To address these challenges, single-molecule electronics has emerged over the past decades and has demonstrated functional elements including molecular diodes,[125] molecular switches,[126] memory device,[127] bio- and chemical sensors,[128] and molecular transistors.[129] Conjugated molecules typically serve as the active building blocks, and hydrocarbon π systems and other light-element analogues featuring pπ–pπ conjugation have been widely explored in numerous single-molecule charge transport studies.[130] Within the carbolong framework, incorporation of a metal center chelated by multiple carbon atoms establishes dπ–pπ conjugation, modifies frontier orbital alignment and transmission pathways, and confers aromatic stabilization and chemical robustness. Accordingly, elucidating charge transport through dπ–pπ frameworks in carbolong complexes is essential for identifying faster and more efficient transmission concepts and for broadening the scope of single-molecule electronics. Relative to conventional metallaaromatics, such as metallabenzenes, carbolong frameworks present a single, linear metal–carbon conduction path with strong dπ–pπ delocalization and superior chemical stability.[29,83] This architecture supports reproducible single-molecule conductance, clean protonation-controlled rectification, and robust chemical stability under bias. In contrast, many previously reported metallaaromatic molecules rely on aryl-based ligand frameworks, where rotation between aromatic units and changes in substituents significantly alter conjugation and energy-level alignment, leading to variable molecule–electrode coupling and broad conductance distributions.[131]

Construction of a metal-molecule-metal junction device using break junction (BJ) techniques provides a robust approach for characterizing the electrical conductance of individual molecules

View Article Online
DOI: 10.1039/D5NR05504K

and elucidating the charge transport mechanisms at the molecular scale.[132] Mechanically controlled break junction[133] (MCBJ) and scanning tunneling microscope break junction[134] (STMBJ) are widely adopted BJ techniques. In both methods, a single molecule bridges two metal electrodes that are gradually separated until the junction ruptures. Conductance is extracted from the resulting conductance *vs* junction separation traces and statistical analyses, which reveal the most probable conductance of a single molecule. These approaches enable detailed evaluation of the impact of dπ–pπ conjugation on electron transport.

Primarily attributed to the quantum interference effect, the conductance of single-molecule junctions is contingent upon the connecting sites and the charge transport pathway within the aromatic system.[135] While in carbolong metallaaromatic compounds, dπ–pπ conjugated aromatic rings regulates charge transport through the molecular bridge by unique electron delocalization. The investigation of charge transport through carbolong complexes at the single-molecule level was only made possible recently by Li et al.,[59] using MCBJ technique. They measured three Osmium (Os)-centered alkene carbolong complexes **2**, **3**, and **4** shown in **Figure 2a - 2c**. As shown in the one-dimensional (1D) conductance histograms, the conductance of complex **2** is higher than complex **3** by almost one order of magnitude. The conductance of complex **4** only shows an exponential drop without any molecular plateau features (**Figure 2d**), implying a conductance lower than the detection limitation. Compared to complex 4, the osmafuran unit in complex **2** and **3** contributes to a more delocalized structure due to a higher planarity with the fused lactone ring. The opened osmafuran also disrupts the electronic delocalization through the molecular backbone, forcing the charge to migrate through an oxygen atom with a weaker conjugation, thereby resulting a lower conductance. Meanwhile, side chain engineering is commonly used to alter the molecular conductance by manipulating the orbital alignment. In complex **3**, due to destructive quantum interference effect, charge transport prefers path through the carbon chain around the metalacyclic ring rather than through the metal-carbon carbene bond. The phosphonium group in complex **2**, however, enhanced the carbene character of the Os-C double bond by involving the resonant structure, leading to a higher degree of electron delocalization. These findings indicate that the conductance of carbolong complexes is predominantly governed by the dπ–pπ conjugation which can be effectively tuned by manipulating in the main conjugation backbone and/or side group.

View Article Online
DOI: 10.1039/D5NR05504K

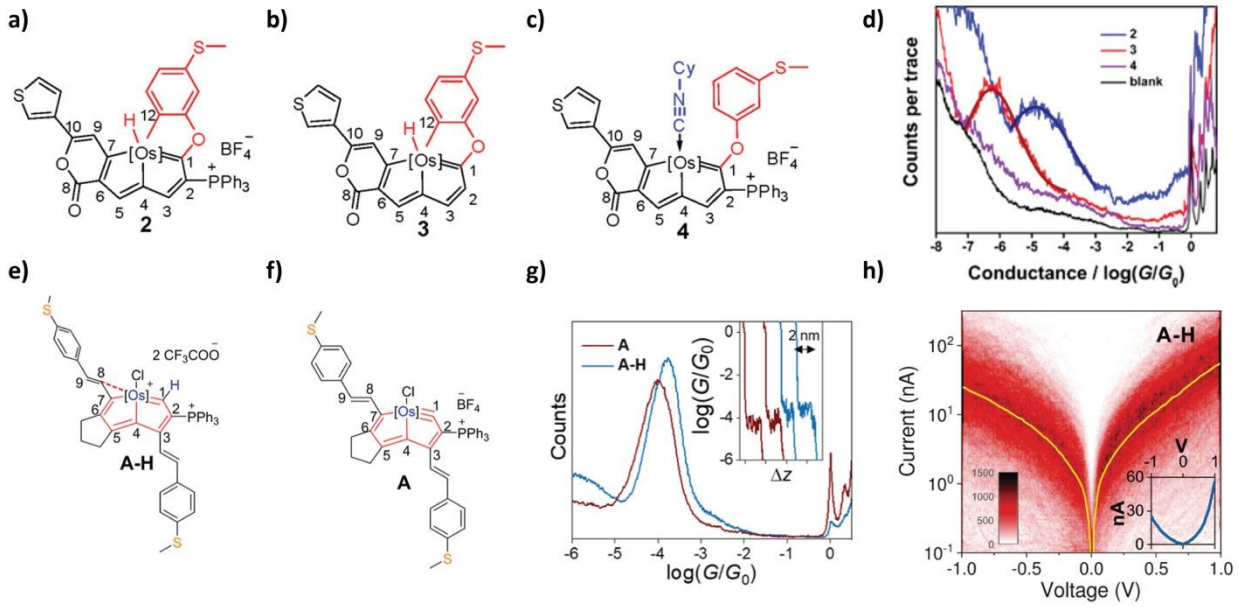

Figure 2. (a)-(c) Structures of carbolong complex **2**, **3**, and **4**. (d) Conductance histograms of carbolong complexes. Reproduced with permission from Ref. 57. *Copyright 2017 American Chemical Society.* (e) and (f) Molecular structure of carbolong complex A-H and A. (g) Conductance histograms of A and A-H. (h) IV measurements of A and A-H. Reproduced with permission from Ref. 58. *Copyright 2023 American Chemical Society.*

Besides the metal-carbon carbene bond, the metallocarbyne carbolong complex has also exhibited potential for molecular electronic devices due to stronger connectivity between the metal atom and carbon atoms. Owing to the *d*-orbital electron activity, metal atom can participate in multiple bonding reactions, including distinct secondary interactions. For example, the hyperconjugation effect from the metal-carbon center enhances aromaticity for the main molecular backbone and offers an additional way for charge transport. Using STMBJ technique, Tang et al.[87] recently investigated the molecular conductance of metallpentacarbyne based carbolong complex A (shown in **Figure 2f**), including the osmium-carbon triple bond in the central fused ring. The osmium-embedded carbolong carbyne complex yields a higher conductance than their pπ-pπ conjugated counterparts. Moreover, the metal carbyne bond can be protonated to a metal carbene bond, which enables the hyperconjugation with the secondary interaction induced by the metal atom. Although the unprotonated carbyne complex has a higher degree of planarity, the protonated carbolong complex A-H (**Figure 2e**) exhibits higher transmission efficiency. Due to σ-type interaction with protonated hydrocarbon, the Os-*d* xy orbital from the metal atom is further stabilized, which facilitates an energy-level crossing between the LUMO and LUMO+1. Consequently, the osmium center exhibits enhanced electron-accepting character, leading to stronger interactions with the neighboring carbon atoms. The compact A-H molecule renders a twisting angle between the C7-C8 bond and the metal center, causing a smaller spatial gap between the C8 and the osmium atom. The reduced gap makes it possible for charge transport through space rather than through bonds in the molecule, which enhances the conductance of the protonated A-H complex (**Figure 2g**). Furthermore, as shown in **Figure 2h**, complex A-H shows an asymmetric I-V behavior, a signature of rectification effect, contrasting the symmetric I-V curve of unprotonated complex A. DFT

View Article Online
DOI: 10.1039/D5NR05504K

calculations suggest that the frontier molecular orbital (FMO) of complex A is evenly distributed through the whole backbone, but complex A-H exhibits a more localized FMO resulting from protonation. Since the LUMO of A-H is closer to one of the anchors, this asymmetric orbital distribution facilitates bias-dependent transmission, leading to higher current in the forward bias direction and more suppressed electron transmission in the reverse bias region. Therefore, chemically tailoring transition metal through hyperconjugation represents a promising strategy for regulating charge flow in metallaaromatic molecules.

3.2 Application in solar cells

Solar cells are photovoltaic devices that convert sunlight directly into electricity.[136] To address resource constraints, environmental pollution, and the inefficiencies of fossil-fuel power generation, photovoltaic technologies have been commercialized and are expected to play a central role in the energy transition and storage landscape. The conversion of solar energy to electrical power proceeds through three steps, namely absorption and exciton generation, charge separation, and carrier collection at the electrodes.[137] Carbolong complexes are promising electron-transport layers in both OSCs and PSCs because metal–carbon multiple-bond dπ–pπ conjugation enhances through-backbone transmission within a metallaaromatic framework.[54] Their aromatic stabilization also promotes chemical robustness, which can extend operating lifetime at high efficiency. Taken together, carbolong complexes could be potential electron transport layer (ETL) candidates for next-generation energy-conversion devices due to their improved performance.

Over the past few decades, OSCs have garnered broad attention owing to their lightweight nature, mechanical flexibility, solution processability, and potential for low-cost manufacturing.[138] These non-fullerene acceptors OSCs typically adopt an acceptor–donor–acceptor molecular architecture with π-conjugated linkers, which enables efficient charge separation and transport. However, such conjugated frameworks are chemically vulnerable when interfaced with low-work-function interlayers or basic cathode interfacial materials (CIMs).[139] Undesirable chemical interactions at these interfaces can induce structural or electronic degradation of the non-fullerene acceptors, leading to reduced device efficiency and poor operational stability. As a result, the long-term performance of OSCs is often limited by the chemical instability of non-fullerene acceptors in contact with CIMs. Because the photovoltaic efficiency of OSCs critically depends on preserving the electronic integrity of the acceptor materials, the development of CIMs that combine effective energy-level alignment with high structural and chemical stability is essential for realizing commercially viable, long-lived OSC devices.

View Article Online
DOI: 10.1039/D5NR05504K

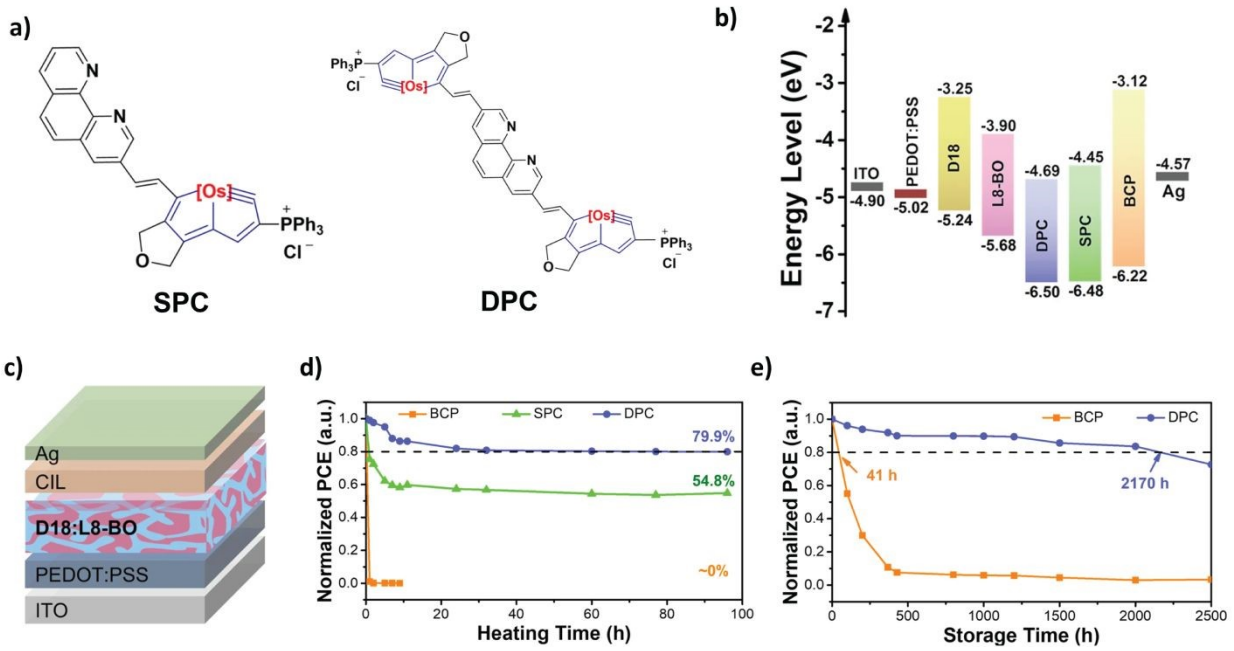

Figure 3. (a) Molecular structures of SPC and DPC. (b) The energy levels of the functional layer with different materials in OSC. (c) Device structure of single junction OSC. (d) The thermal stability of devices with bathocuproine, SPC and DPC cathode interlayers. (e) The storage lifetime of devices with bathocuproine and DPC cathode interlayers. Reproduced with permission from Ref. 116. *Copyright 2023 Springer Nature.*

Previous works have validated that metallic chelation can create high-stability CIMs with improved photovoltaic performance.[55,89,140] Thus, polydentate metal-carbon chelated carbolong compounds are promising candidates for novel CIMs in OSCs. Recently, Lai et al.[121] reported two carbolong based alcohol-soluble CIMs, single-phenanthroline-carbolong (SPC) and double-phenanthroline-carbolong (DPC). As shown in **Figure 3a**, for stabilizing the metal atoms, they adopted the same phenanthroline group as a multi-functional chelating agent connected with one and two carbolong metallapentalene complex(s), respectively. Due to the π delocalization between the phenanthroline and introduced carbolong substitution, both SPC and DPC exhibit lower HOMO and LUMO compared to the commonly used CIM bathocuproine. Lower HOMO of SPC and DPC can potently hinder the transmission of hole carriers from the active layer to the cathode avoiding the recombination with electrons. On the other hand, the decreased LUMO level is closer to the work function of cathode material Ag, which boosts the charge transport at the interface between the active layer and the ETL (**Figure 3b**). As a result, the efficiencies of OSCs with SPC and DPC are improved to 17.8% and 18.2%, respectively. Moreover, DPC effectively inhibits the chemical reaction between the cathode interlayer and acceptor on account of powerful electron-withdrawing properties and large steric hindrance. Consequently, DPC-based devices retain approximately 80% of their initial efficiency after 96 h of thermal aging at 85 °C (**Figure 3d**) and exhibit an extended storage T_{80} lifetime of about 2170 h in the dark (**Figure 3e**). Under illumination, DPC-based devices also exhibit enhanced operational stability. This improvement is attributed to the chemically robust and sterically hindered DPC interlayer, which mitigates interfacial degradation at the cathode and thereby prolongs device lifetime.

View Article Online
DOI: 10.1039/D5NR05504K

In addition, organic-inorganic halide PSCs, as another key branch of photovoltaic devices, attract enormous interest due to their superb light absorption properties, ease of fabrication, low cost, and low carrier recombination rates.[141] Previous works have demonstrated that the embedded π conjugation between donor and accepter can optimize the electron transportation to the ETL by applying dipole moments at the interface of perovskite and ETL.[89] Recently, Wang et al.[140] introduced a series of carbolong-derived complexes as cathode interlayer in reverted PSCs. Owing to the dipole moments of carbolong derivatives, the work function of cathode materials (e.g., Ag and Au) coated with carbolong molecules can be significantly decreased, enhancing electron transport from ETL to external metal cathode. Therefore, using carbolong-derived complexes, the inverted PSCs reached a power conversion efficiency as high as 21.29%. Another recent work also explored integrating carbolong complexes as an electron-transfer bridge to enhance the interaction between perovskite films and C60 layers. An increased efficiency up to 25.80% with long-term stability was observed.[142] Conclusively, the incorporation of carbolong complexes enhances solar-cell performance by simultaneously stabilizing the cathode interface and optimizing interfacial charge extraction. Compared with conventional organic cathode interfacial materials such as bathocuproine, carbolong-based interlayers exhibit downshifted HOMO and LUMO energy levels, which suppress hole leakage and interfacial recombination. At the same time, their LUMO levels align more favorably with the cathode Fermi level, enabling more efficient electron extraction and improved operational stability.

4. Photoresponsive Applications

Metal *d*-orbital participation in dπ–pπ conjugation narrows the HOMO–LUMO gap in carbolong complexes, which produces broad absorption.[49,54] As a result, these complexes exhibit favorable charge-transport characteristics and pronounced photoresponsive behavior, including photothermal conversion,[143] photoluminescent,[49] and photoacoustic effect.[144] The broad and intense UV–vis–NIR bands enable efficient photothermal heating that has been applied to phase-transition materials,[143] self-healing devices,[145] shape memory materials,[57] and phototherapy.[146] In this section we use photoresponsive to denote light-induced thermal, optical, or mechanical changes in carbolong materials. Zhu et al.[92] first synthesized the 12C carbolong complex (**Figure 4a**), where all chelating agents are carbon atoms in the equatorial plane. The resulting strong metal–carbon conjugation and high thermodynamic stability give rise to a broad and tunable absorption band spanning the UV–vis to near-infrared region. Owing to this broad NIR absorption, the 12C carbolong complex exhibits efficient and stable photothermal conversion, enabling its application in photothermal cancer therapy. When formulated into polymeric micelles and intravenously injected into tumor-bearing mice, the carbolong derivatives accumulate at the tumor site and generate sufficient localized heating under NIR irradiation. As shown in **Figure 4b**, this photothermal treatment leads to pronounced tumor regression, with near-complete tumor elimination observed within 14 days.

View Article Online
DOI: 10.1039/D5NR05504K

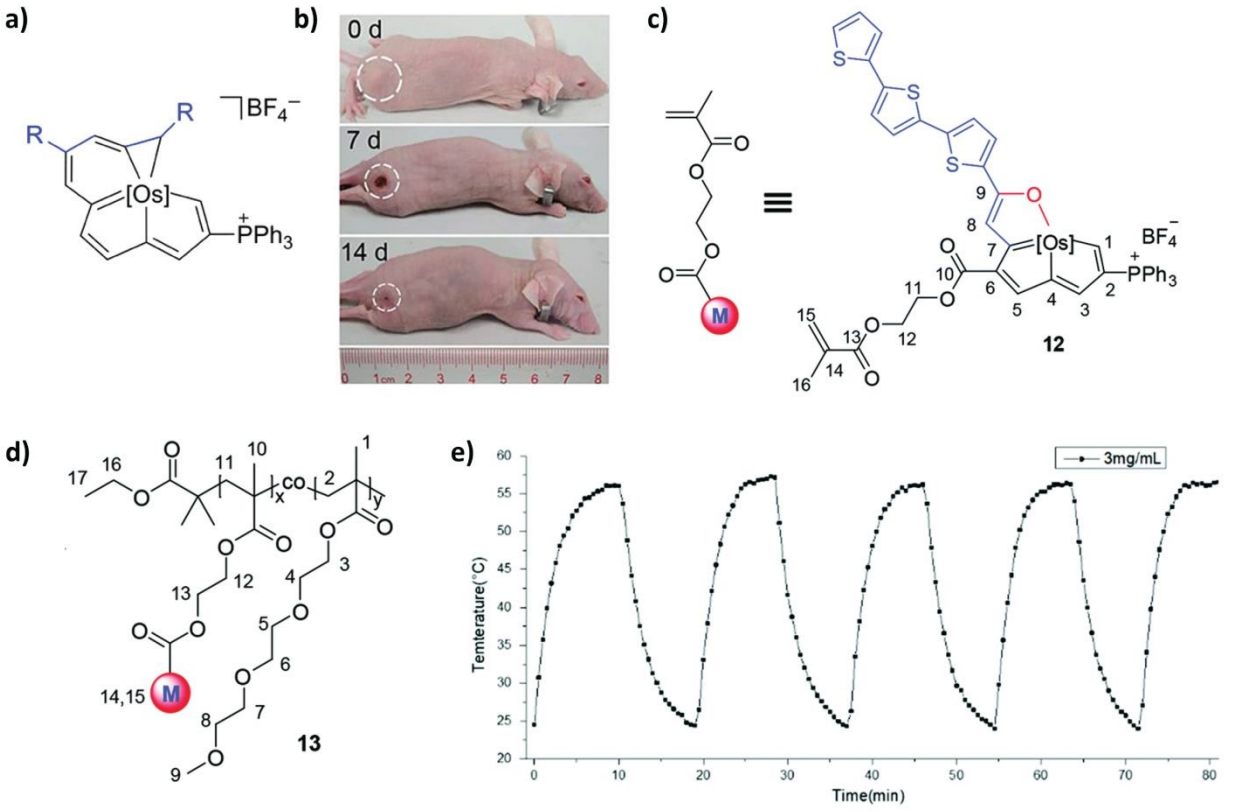

Figure 4. (a) Molecular structures of 12C carbolong complex. (b) Regression of the tumor after injection of carbolong derivatives. Reproduced with permission from Ref. 88. *Copyright 20*16 *American Association for the Advancement of Science.* (c) Molecular structure of osmapentalenofuran **12**. (d) Metallopolymer **13** structure. (e) Temperature curves of carbolong-based polymer **13** with five laser on-off cycles. Reproduced with permission from Ref. 137. *Copyright 20*18 *Royal Society of Chemistry.*

In addition, the integration of carbolong complexes into polymeric architectures has catalyzed significant interest in metallopolymers within the fields of polymer sciences. For instance, Lu et al.[143] in 2018 reported a metallopolymer **13**, a system derived based on osmapentalenofuran (**Figure 4c** and **4d)**. Owing to the strong metal–carbon conjugation and extended π-system of the carbolong motif, polymer **13** exhibits efficient NIR light absorption and rapid photothermal conversion. Under 808 nm laser irradiation (1.0 W cm^{-2}), an aqueous solution of polymer **13** shows a temperature increase of approximately 34 °C within 8 min. The photothermal response remains stable over multiple laser on–off cycles, demonstrating excellent photothermal durability (**Figure 4e**). In a parallel effort, Zhang et al.[147] developed NIR photothermally healable carbolong polyurethanes (CLPUs) based on the 12C carbolong framework (**Figure 5a-c**). The broad UV–vis–NIR absorption of the carbolong units enables efficient photothermal conversion, with the heating efficiency readily tuned by varying the fraction of carbolong moieties incorporated into the polymer backbone (**Figure 5d**). Upon NIR irradiation, the localized photothermal heating activates polymer chain mobility at the damaged regions, allowing rapid (< 30 s) and repeatable (> 5 cycles) self-healing with precise spatial and temporal control (**Figure 5e**). Together, these studies demonstrate that carbolong motifs can serve as robust photothermal transducers within polymer matrices, providing a versatile platform for adaptive and self-healing polymeric materials.

View Article Online
DOI: 10.1039/D5NR05504K

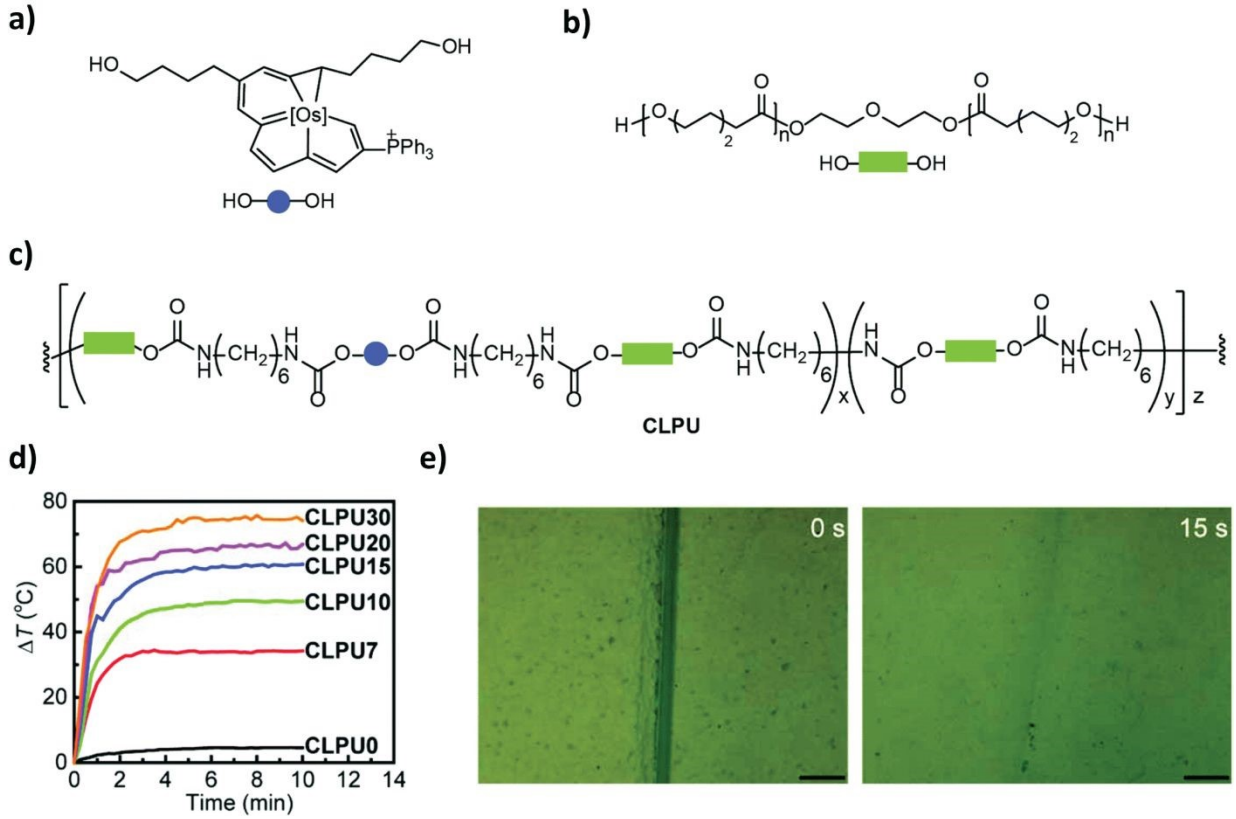

Figure 5. (a) Carbolong polyurethanes structure. (b) Ploymerizable groups structure. (c) Molecular structures of CLPU containing (a) and (b). (d) The increase of temperature with varying carbolong content in CLPU. (e) Optical images of the healing process after 15 seconds. Reproduced with permission from Ref. 141. *Copyright 2019 Royal Society of Chemistry.*

As evidenced by the aforementioned studies, the distinctive chemical and physical properties arising from the metal *d* orbital endow carbolong complexes with superior photothermal and photosensitive properties. These traits not only underscore their burgeoning potential in materials science and biomedical treatments but also position them as compelling candidates in future optoelectronics and thermoelectric molecular devices.

Building on the synthesis–property–application correlations summarized above, recent advances have transitioned carbolong chemistry from a fundamental molecular class into a versatile functional platform. While broad synthetic access has only been realized within the last decade, enabled by stepwise chain-growth and one-pot multiyne chelation strategies, these methodologies now facilitate the gram-scale production of stable frameworks across Os, Ru, Rh, and Ir.[112,148] Although device-level integration remains in its nascent stages, current results establish clear advantages when carbolong complexes are embedded into functional architectures. These include robust photothermal responses, efficient interfacial electron transport, high single-molecule conductance, and compatibility with stable, self-healing elastomers. These recent findings indicate significant scope for carbolong-based electronics, energy harvesting, and biomedical technologies,

View Article Online
DOI: 10.1039/D5NR05504K

necessitating systematic investigations that bridge molecular design with device-level performance metrics.

5. Conclusion and Outlook

Emerging as a distinct class of compounds with metallaaromaticity, carbolong complexes exhibit exceptional features such as rare Craig aromaticity, providing enhanced stability, extensive electron transmission, broad absorption, and photothermal characteristics. We have concluded various synthesis methods, novel molecular designs, optoelectronics applications, and photoresponsive applications of carbolong complexes. The synthesis and design strategies have allowed more accessible and faster carbolong complex fabrication with a high yield, which supports deeper fundamental investigation in physics and chemistry, and broader application exploration for catalysis, molecular optoelectronics, energy conversion, and biomedicines. In addition, as discussed in this review, the nature of the unique dπ-pπ conjugation from the embedded metal atom positions carbolong complexes as promising candidates for improving the technology in nanoelectronics, energy conversion, optoelectronics, biomedicine, and intelligent materials.

Looking forward, the future of carbolong chemistry appears vibrant and full of potential. On the synthetic side, progress will come from five aspects: i) varying the metal center (Os, Ru, Rh, Ir) to tune redox windows and spin–orbit coupling;[110–112] ii) lengthening or fusing the carbon backbone to enforce full sp^2 conjugation and narrow the gap;[149] iii) tailoring ancillary ligands and terminal anchors to adjust interfacial dipoles and contact geometry and coupling;[150] iv)introducing core protonation or redox switches to modulate conductance and work function while retaining conjugation;[60] v) developing polymerizable or nanographene hybrid carbolong to yield stable and scalable films;[147] vi) the fused 15C framework **20** featuring D_{5h} symmetry is promising building block for π conjugated functional molecules and may be considered as a metal-doped graphene fragment.[109] The dπ–pπ conjugation enables intriguing charge transport and presents opportunities for single-molecule electronics within metallaaromatic systems, particularly those exhibiting Craig-type aromaticity or antiaromaticity. Tunable charge pathways in carbolong molecular junctions point to advances in molecular switches, diodes, and sensors. The application of carbolong complexes in organic and perovskite solar cells signals a shift toward clean and highly efficient energy-conversion devices. As research progresses, optimizing and tailoring carbolong derivatives for interlayer and interface design will likely open new frontiers in solar energy technology. Their photothermal and photosensitive properties also suggest promising applications in materials science and biomedical treatment. These design levers translate directly to function by controlling single-molecule transport, stabilizing and aligning interfaces in OSC and PSC interlayers, and setting the optical bandwidth that underpins photothermal and other photoresponsive uses, thereby linking molecular edits to device performance.

Translating these opportunities into practical technologies requires attention to several challenges. First, interfacial and operational stability must be demonstrated under illumination, heat, humidity, and bias, since low-work-function contacts can induce parasitic reactions and energy-level drift. Second, control and reproducibility of the electrical contact remain difficult in single-molecule and thin-film platforms. Variations in anchor geometry, local environment, and electrode coupling

View Article Online
DOI: 10.1039/D5NR05504K

can mask intrinsic transport. Third, scalable processing must deliver continuous and oriented films with minimal defects such that charge extraction and optical response are preserved during manufacturing. Addressing these issues in concert with the design levers above will create a clear path from molecular discovery to reliable devices.

Finally, this article captures the current state of carbolong chemistry and propels it into a future where these complexes stand poised to make significant contributions across a spectrum of scientific and technological domains on the molecular scale. Investigation is encouraged to delve deeper into the synthesis, design, and applications of carbolong complexes, fostering innovation and shaping the landscape of cutting-edge materials and molecular devices.

View Article Online
DOI: 10.1039/D5NR05504K

Author contributions

H.Z. and S.C. conceived the project under the guidance of K.W. H.Z. and S.C. performed the analysis and drafted the manuscri pt in collaboration with K.W. All the authors have reviewed the manuscript.

Conflicts of interest

There are no conflicts to declare.

Data availability

Data sharing not applicable to this article as no datasets were generated or analyzed during the current study.

Acknowledgements

We gratefully thank the financial support from the U.S. Department of Energy, Office of Science, Basic Energy Sciences under Award No. DE-SC0024924 (Conceptualization, analysis, and drafting). K.W. also acknowledges the support from the University of Miami Provost's Research Award (UM-PRA-2025-5714). S.C. acknowledges the support from the National Natural Science Foundation of China (Nos. 22305113 and 22350009).

View Article Online
DOI: 10.1039/D5NR05504K

Reference

1. W. A. Hofmann, *Proc. R. Soc. Lond.*, 1857, **8**, 1–3.

2. P. von Ragué Schleyer, *Chem. Rev.*, 2001, **101**, 1115–1117.

3. P. von Ragué Schleyer, *Chem. Rev.*, 2005, **105**, 3433–3435.

4. A. T. Balaban, P. v. R. Schleyer and H. S. Rzepa, *Chem. Rev.*, 2005, **105**, 3436–3447.

5. A. Sekiguchi, T. Matsuo and H. Watanabe, *J. Am. Chem. Soc.*, 2000, **122**, 5652–5653.

6. K. Parmar, C. S. Blaquiere, B. E. Lukan, S. N. Gengler and M. Gravel, *Nat. Synth.*, 2022, **1**, 696–700.

7. N. M.-W. Wu, M. C. Warndorf, A. Alexander-Katz and T. M. Swager, *Macromolecules*, 2024, **19**, 41.

8. J. Mei, D. H. Kim, A. L. Ayzner, M. F. Toney and Z. Bao, *J. Am. Chem. Soc.*, 2011, **133**, 20130–20133.

9. T. Lei, Y. Cao, Y. Fan, C. J. Liu, S. C. Yuan and J. Pei, *J. Am. Chem. Soc.*, 2011, **133**, 6099–6101.

10. J. Huang, Z. Mao, Z. Chen, D. Gao, C. Wei, W. Zhang and G. Yu, *Chem. Mater.*, 2016, **28**, 2209–2218.

11. A. B. Okey, D. S. Riddick and P. A. Harper, *Trends Pharmacol. Sci.*, 1994, **15**, 226–232.

12. E. A. Meyer, R. K. Castellano and F. Diederich, *Angew. Chem. Int. Ed.*, 2003, **42**, 1210–1250.

13. T. Kawakami, K. Murakami and K. Itami, *J. Am. Chem. Soc.*, 2015, **137**, 2460–2463.

14. X. Liu, M. He, D. Calvani, H. Qi, K. B. S. S. Gupta, H. J. M. de Groot, G. J. A. Sevink, F. Buda, U. Kaiser and G. F. Schneider, *Nat. Nanotechnol.*, 2020, **15**, 307–312.

15. A. S. Dias, S. Lima, M. Pillinger and A. A. Valente, *Wiley-VCH*, 2010, **165–186.**

16. J. P. Lange, E. van der Heide, J. van Buijtenen and R. Price, *ChemSusChem*, 2012, **5**, 150–166.

17. R. J. van Putten, J. C. van der Waal, E. de Jong, C. B. Rasrendra, H. J. Heeres and J. G. de Vries, *Chem. Rev.*, 2013, **113**, 1499–1597.

18. W. Chen, H. Li, J. R. Widawsky, C. Appayee, L. Venkataraman and R. Breslow, *J. Am. Chem. Soc.*, 2014, **136**, 918–920.

19. Z. Xie, X. L. Ji, Y. Song, M. Z. Wei and C. K. Wang, *Chem. Phys. Lett.*, 2015, **639**, 131–134.

20. L. J. Karas and J. I. C. Wu, Aromaticity, *Elsevier*, 2021, 319–338**.**

21. G. Dai, J. Chang, W. Zhang, S. Bai, K.-W. Huang, J. Xu and C. Chi, *Chem. Commun.*, 2014, **51**, 503–506.

22. Y. Sun, Y. Guo and Y. Liu, *Mater. Sci. Eng. R Rep.*, 2019, **136**, 13–26.

23. S. Fujii, S. Marqués-González, J. Y. Shin, H. Shinokubo, T. Masuda, T. Nishino, N. P. Arasu, H. Vázquez and M. Kiguchi, *Nat. Commun.*, 2017, **8**, 1–8.

24. Z. Jin, Z. F. Yao, K. P. Barker, J. Pei and Y. Xia, *Angew. Chem. Int. Ed.*, 2019, **58**, 2034–2039.

View Article Online
DOI: 10.1039/D5NR05504K

25. H. U. Kim, J. H. Kim, H. Suh, J. Kwak, D. Kim, A. C. Grimsdale, S. C. Yoon and D. H. Hwang, *Chem. Commun.*, 2013, **49**, 10950–10952.

26. Z. Zhang, H. Fan and X. Zhu, *Org. Chem. Front.*, 2017, **4**, 711–716.

27. H. Masui, *Coord. Chem. Rev.*, 2001, **219–221**, 957–992.

28. B. J. Frogley and L. J. Wright, *Chem. Eur. J.*, 2018, **24**, 2025–2038.

29. D. Chen, Y. Hua and H. Xia, *Chem. Rev.*, 2020, **120**, 12994–13086.

30. D. L. Thorn and R. Hoffmann, *Delocalization in metallocycles*, 1979, **3**, 1-1979.

31. G. P. Elliott, W. R. Roper and J. M. Waters, *J. Chem. Soc., Chem. Commun.*, 1982, **811–813.**

32. C. E. F. Rickard, W. R. Roper, S. D. Woodgate and L. J. Wright, *Angew. Chem. Int. Ed.*, 2000, **39**, 750–752.

33. K. C. Poon, L. Liu, T. Guo, J. Li, H. H. Y. Sung, I. D. Williams, Z. Lin and G. Jia, *Angew. Chem. Int. Ed.*, 2010, **49**, 2759–2762

34. T. B. Wen, Z. Y. Zhou and G. Jia, *Collect. Czech. Chem. Commun.*, 2001, **66**, 116.

35. S. M. Ng, X. Huang, T. B. Wen, G. Jia and Z. Lin, *Organometallics*, 2003, **22**, 3898–3904.

36. G. Jia, *Acc. Chem. Res.*, 2004, **37**, 479–486.

37. J. Chen and G. Jia, *Coord. Chem. Rev.*, 2013, **257**, 2491–2521.

38. R. J. Angelici, F. Ruette, N. Valencia, R. Sanchez-Delgado, L. Latos-Grazynski, L. Lisowski, *Organometallics*, 1990, **112**, 14.

39. R. M. Chin and W. D. Jones, *Angew. Chem. Int. Ed.*, 1992, **31**, 357–358.

40. J. R. Bleeke, *Acc. Chem. Res.*, 2007, **40**, 1035–1047.

41. B. J. Frogley and L. J. Wright, *Coord. Chem. Rev.*, 2014, **270–271**, 151–166.

42. H. Wang, X. Zhou and H. Xia, *Chin. J. Chem.*, 2018, **36**, 93–105.

43. Y. Zhang, J. Wei, Y. Chi, X. Zhang, W.-X. Zhang and Z. Xi, *J. Am. Chem. Soc.*, 2017, **139**, 5039–5042.

44. M. Saito and M. Yoshioka, *Coord. Chem. Rev.*, 2005, **249**, 765–780.

45. M. Saito, M. Nakada, T. Kuwabara and M. Minoura, *Chem. Commun.*, 2015, **51**, 4674–4676.

46. Y. Zhang, Y. Chi, J. Wei, Q. Yang, Z. Yang, H. Chen, R. Yang, W.-X. Zhang and Z. Xi, *Organometallics*, 2017, **36**, 2982–2986.

47. X. Zhou, J. Wu, Y. Hao, C. Zhu, Q. Zhuo, H. Xia and J. Zhu, *Chem. Eur. J.*, 2018, **24**, 2389–2395.

48. C. Zhu and H. Xia, *Acc. Chem. Res.*, 2018, **51**, 1691–1700.

49. C. Zhu, S. Li, M. Luo, X. Zhou, Y. Niu, M. Lin, J. Zhu, Z. Cao, X. Lu, T. Wen, Z. Xie, P. v. R. Schleyer and H. Xia, *Nat. Chem.*, 2013, **5**, 698–703.

View Article Online
DOI: 10.1039/D5NR05504K

50. H. Xia, G. He, H. Zhang, T. B. Wen, H. H. Y. Sung, I. D. Williams and G. Jia, *J. Am. Chem. Soc.*, 2004, **126**, 6862–6863.

51. S. Chen, L. Feng, L. Peng, X. Gao, Y. Zhu, L. Yang, D. Chen, K. Zhang, X. Guo, F. Huang and H. Xia, *Angew. Chem. Int. Ed.*, 2023, **62**, e202305489.

52. M. Luo, D. Chen, Q. Li and H. Xia, *Acc. Chem. Res.*, 2023, **56**, 924–937.

53. C. Zhu and H. Xia, *Acc. Chem. Res.*, 2018, **51**, 1691–1700.

54. M. Luo, D. Chen, Q. Li and H. Xia, *Acc. Chem. Res.*, 2023, **56**, 924–937.

55. L. Liu, S. Chen, Y. Qu, X. Gao, L. Han, Z. Lin, L. Yang, W. Wang, N. Zheng, Y. Liang, Y. Tan, H. Xia and F. He, *Adv. Mater.*, 2021, **33**, 2101279.

56. J. Wang, J. Li, Y. Zhou, C. Yu, Y. Hua, Y. Yu, R. Li, X. Lin, R. Chen, H. Wu, H. Xia and H. L. Wang, *J. Am. Chem. Soc.*, 2021, **143**, 7759–7768.

57. L. Yang, P. Ouyang, Y. Chen, S. Xiang, Y. Ruan, W. Weng, X. He and H. Xia, *Giant*, 2021, **8**, 100069.

58. L. Yang, H. Zhao, Y. Xie, P. Ouyang, Y. Ruan, J. Chen, W. Weng, X. He and H. Xia, *Polym. Chem.*, 2022, **13**, 1844–1851.

59. R. Li, Z. Lu, Y. Cai, F. Jiang, C. Tang, Z. Chen, J. Zheng, J. Pi, R. Zhang, J. Liu, Z.-B. Chen, Y. Yang, J. Shi, W. Hong and H. Xia, *J. Am. Chem. Soc.*, 2017, **139**, 14344–14347.

60. C. Tang, X. L. Jiang, S. Chen, W. Hong, J. Li and H. Xia, *J. Am. Chem. Soc.*, 2023, **145**, 10404–10410.

61. M. Faustova, E. Nikolskaya, M. Sokol, M. Fomicheva, R. Petrov and N. Yabbarov, *ACS Appl. Bio Mater.*, 2020, **3**, 8146–8171.

62. N. Lu, Z. Deng, J. Gao, C. Liang, H. Xia and P. Zhang, *Nat. Commun.*, 2022, **13**, 1–11.

63. P. v. R. Schleyer and H. Jiao, *Pure Appl. Chem.*, 1996, **68**, 209–218.

64. T. M. Krygowski, M. K. Cyrański, Z. Czarnocki, G. Häfelinger and A. R. Katritzky, *Tetrahedron*, 2000, **56**, 1783–1796.

65. M. Rosenberg, C. Dahlstrand, K. Kilså and H. Ottosson, *Chem. Rev.*, 2014, **114**, 5379–5425.

66. C. Gunanathan and D. Milstein, *Acc. Chem. Res.*, 2011, **44**, 588–602.

67. T. P. Gonçalves, I. Dutta and K.-W. Huang, *Chem. Commun.*, 2021, **57**, 3070–3082.

68. J. S. Miller and A. J. Epstein, *Angew. Chem. Int. Ed.*, 1994, **33**, 385–415.

69. Z. Xiao, Y. Yuan, Q. Wang, Y. Shao, Y. Bai, Y. Deng, Q. Dong, M. Hu, C. Bi and J. Huang, *Mater. Sci. Eng. R Rep.*, 2016, **101**, 1–38.

70. H. S. Nalwa, *Appl. Organomet. Chem.*, 1991, **5**, 349–377.

71. O. H. Nam, M. D. Bremser, B. L. Ward, R. J. Nemanich and R. F. Davis, *Part 2*, 1997, **36**, 532.

72. M. P. Coogan, P. J. Dyson and M. Bochmann, *Organometallics*, 2012, **31**, 5671–5672.

View Article Online
DOI: 10.1039/D5NR05504K

73. M. Patra and G. Gasser, *ChemBioChem*, 2012, **13**, 1232–1252.

74. E. V. Vinogradova, *Pure Appl. Chem.*, 2017, **89**, 1619–1640.

75. G. W. Parshall, R. E. Putscher, K. Ziegler, G. Natta, G. Wilkinson and E. Fischer, *J. Chem. Educ.*, 1986, **63**, 189-191.

76. G. W. Parshall, *Organometallics* 1987, **6**, 687–692**.**

77. B. M. Gardner, C. C. C. Johansson Seechurn and T. J. Colacot, *Wiley*, 2020, **1–22.**

78. D. P. Craig and N. L. Paddock, *Nature*, 1958, **181**, 1052–1053.

79. E. Hückel, Quantentheoretische Beiträge zum Benzolproblem, I. Die Elektronenkonfiguration des Benzols und verwandter Verbindungen, *Z. Phys.*, 1931, **70**, 204–286.

80. D. Chen, Q. Xie and J. Zhu, *Acc. Chem. Res.*, 2019, **52**, 1449–1460.

81. D. Chen, Y. Hua and H. Xia, *Chem. Rev.*, 2020, **120**, 12994–13086.

82. C. Zhu, C. Yang, Y. Wang, G. Lin, Y. Yang, X. Wang, J. Zhu, X. Chen, X. Lu, G. Liu and H. Xia, *Sci. Adv.*, 2016, **2**, 1.

83. X. Zhou and Q. Zhuo, *Chin. J. Chem.*, 2025, **44**, 583–603.

84. S. Chen, C. Cao, Z. Yu, A. Zhang, X. Lai, L. Peng, Y. Hua, L. Yang, W. Jiang, D. Chen, Z. Wang, F. He and H. Xia, *Adv. Funct. Mater.*, 2023, **33**, 2300359.

85. Z. Lu, Q. Lin, Y. Cai, S. Chen, J. Chen, W. Wu, X. He and H. Xia, *ACS Macro Lett.*, 2018, **7**, 1034–1038.

86. Z. Lu, Y. Cai, Y. Wei, Q. Lin, J. Chen, X. He, S. Li, W. Wu and H. Xia, *Polym. Chem.*, 2018, **9**, 2092–2100.

87. C. Tang, X. L. Jiang, S. Chen, W. Hong, J. Li and H. Xia, *J. Am. Chem. Soc.*, 2023, **145**, 10404–10410.

88. Q. Li, Y. Hua, C. Tang, D. Chen, M. Luo and H. Xia, *J. Am. Chem. Soc.*, 2023, **145**, 7580–7591.

89. S. Chen, L. Liu, X. Gao, Y. Hua, L. Peng, Y. Zhang, L. Yang, Y. Tan, F. He and H. Xia, *Nat. Commun.*, 2020, **11**, 1–11.

90. C. Yang, G. Lin, C. Zhu, X. Pang, Y. Zhang, X. Wang, X. Li, B. Wang, H. Xia and G. Liu, *J. Mater. Chem. B*, 2018, **6**, 2528–2535.

91. X. He, X. He, S. Li, K. Zhuo, W. Qin, S. Dong, J. Chen, L. Ren, G. Liu and H. Xia, *Polym. Chem.*, 2017, **8**, 3674–3678.

92. C. Zhu, C. Yang, Y. Wang, G. Lin, Y. Yang, X. Wang, J. Zhu, X. Chen, X. Lu, G. Liu and H. Xia, *Sci. Adv.*, 2016, **2**, 1.

93. M. Faraday, *Philos. Trans. R. Soc. Lond.*, 1825, **115**, 440–466.

94. B. Brutschy, *Chem. Rev.*, 2000, **100**, 3891–3920.

95. E. L. Spitler, C. A. Johnson and M. M. Haley, *Chem. Rev.*, 2006, **106**, 5344–5386.

View Article Online
DOI: 10.1039/D5NR05504K

96. Y. Ouyang, X. H. Xu and F. L. Qing, *Angew. Chem. Int. Ed.*, 2022, **61**, e202114048.

97. R. Taylor and D. R. M. Walton, *Nature*, 1993, **363**, 685–693.

98. T. M. Krygowski, M. K. Cyrański, Z. Czarnocki, G. Häfelinger and A. R. Katritzky, *Tetrahedron*, 2000, **56**, 1783–1796.

99. R. H. Mitchell, *Chem. Rev.*, 2001, **101**, 1301–1315.

100. T. M. Krygowski and M. K. Cyrański, *Chem. Rev.*, 2001, **101**, 1385–1419.

101. Q. Zhuo, J. Lin, Y. Hua, X. Zhou, Y. Shao, S. Chen, Z. Chen, J. Zhu, H. Zhang and H. Xia, *Nat. Commun.*, 2017, **8**, 1–7.

102. C. Zhu, M. Luo, Q. Zhu, J. Zhu, P. v. R. Schleyer, J. I. C. Wu, X. Lu and H. Xia, *Nat. Commun.*, 2014, **5**, 1–7.

103. M. Luo, L. Long, H. Zhang, Y. Yang, Y. Hua, G. Liu, Z. Lin and H. Xia, *J. Am. Chem. Soc.*, 2017, **139**, 1822–1825.

104. C. Zhu, Y. Yang, J. Wu, M. Luo, J. Fan, J. Zhu and H. Xia, *Angew. Chem. Int. Ed.*, 2015, **54**, 7189–7192.

105. C. Zhu, Y. Yang, I. Luo, A. Yang, J. Wu, L. Chen, G. Liu, T. Wen, H. Xia, C. Z. Hu, Y. Yang, M. Luo, J. Wu, L. Chen, T. W. En, J. Zhu, H. Xia, C. Yang and G. L. Iu, *Angew. Chem. Int. Ed.*, 2015, **54**, 6181–6185.

106. K. Zhuo, Y. Liu, K. Ruan, Y. Hua, Y. M. Lin and H. Xia, *Nat. Synth.*, 2022, **2**, 67–75.

107. C. Zhu, J. Wu, S. Li, Y. Yang, J. Zhu, X. Lu and H. Xia, *Angew. Chem. Int. Ed.*, 2017, **56**, 9067–9071.

108. C. Zhu, X. Zhou, Q. Zhu, Y. Yang, T. Bin Wen, H. Xia, D. Zhu, D. Zhu, X. Zhou, Q. Zhu, Y. Yang and D. B. en, *Angew. Chem.*, 2018, **130**, 3208–3211.

109. B. Xu, D. Chen, K. Ruan, M. Luo, Y. Cai, J. Qiu, W. Zhou, B. Cao, Z. Lin, J. L. Sessler and H. Xia, *Nature*, 2025, **641**, 106–111.

110. Q. Zhuo, H. Zhang, Y. Hua, H. Kang, X. Zhou, X. Lin, Z. Chen, J. Lin, K. Zhuo and H. Xia, *Sci. Adv.*, 2018, **4**, 336–358.

111. J. Guo, Z. Lu, W. Zhou, Q. Zhuo, D. Chen and H. Xia, *Inorg. Chem. Front.*, 2025, **12**, 7226.

112. J. Li, Z. Chu, Z. Lu, M. Luo, D. Chen and H. Xia, *Organometallics*, 2022, **41**, 2589–2596.

113. Q. Zhuo, H. Zhang, L. Ding, J. Lin, X. Zhou, Y. Hua, J. Zhu and H. Xia, *iScience*, 2019, **19**, 1214–1224.

114. J. Li, Q. Zhuo, K. Zhuo, D. Chen and H. Xia, *Acta Chim. Sin.*, 2021, **79**, 71.

115. Z. Lu, Q. Lin, Y. Cai, S. Chen, J. Chen, W. Wu, X. He and H. Xia, *ACS Macro Lett.*, 2018, **7**, 1034–1038.

116. C. Yang, G. Lin, C. Zhu, X. Pang, Y. Zhang, X. Wang, X. Li, B. Wang, H. Xia and G. Liu, *J. Mater. Chem. B*, 2018, **6**, 2528–2535.

View Article Online
DOI: 10.1039/D5NR05504K

117. J. Li, J. Wang, Y. Zhou, C. Yu, H. Liu, X. Qi, R. Li, Y. Hua, Y. Yu, R. Chen, D. Chen, L. Mao, H. Xia and H. L. Wang, *Mater. Chem. Front.*, 2022, **6**, 2211–2218.

118. N. Xin, J. Guan, C. Zhou, X. Chen, C. Gu, Y. Li, M. A. Ratner, A. Nitzan, J. F. Stoddart and X. Guo, *Nat. Rev. Phys.*, 2019, **1**, 211–230.

119. C. Tang, M. Shiri, H. Zhang, R. T. Ayinla and K. Wang, *Nanomaterials*, 2022, **12**, 698.

120. H. Zhang, M. Shiri, R. T. Ayinla, Z. Qiang and K. Wang, *MRS Commun.*, 2022, **12**, 495–509.

121. X. Lai, S. Chen, X. Gu, H. Lai, Y. Wang, Y. Zhu, H. Wang, J. Qu, A. K. K. Kyaw, H. Xia and F. He, *Nat. Commun.*, 2023, **14**, 1–11.

122. H. Liu, Z. Lu, W. Zhang, J. Wang, Z. Lu, Q. Dai, X. Qi, Y. Shi, Y. Hua, R. Chen, T. Shi, H. Xia and H. L. Wang, *Adv. Sci.*, 2022, **9**, 2203640.

123. J. Li, J. Wang, Y. Zhou, C. Yu, H. Liu, X. Qi, R. Li, Y. Hua, Y. Yu, R. Chen, D. Chen, L. Mao, H. Xia and H. L. Wang, *Mater. Chem. Front.*, 2022, **6**, 2211–2218.

124. C. E. Leiserson, N. C. Thompson, J. S. Emer, B. C. Kuszmaul, B. W. Lampson, D. Sanchez and T. B. Schardl, *Science*, 2020, **368**, 1-7.

125. B. Capozzi, J. Xia, O. Adak, E. J. Dell, Z. F. Liu, J. C. Taylor, J. B. Neaton, L. M. Campos and L. Venkataraman, *Nat. Nanotechnol.*, 2015, **10**, 522–527.

126. C. D. Frisbie, *Science*, 2016, **352**, 1394–1395.

127. T. Miyamachi, M. Gruber, V. Davesne, M. Bowen, S. Boukari, L. Joly, F. Scheurer, G. Rogez, T. K. Yamada, P. Ohresser, E. Beaurepaire and W. Wulfhekel, *Nat. Commun.*, 2012, **3**, 1–6.

128. S. Dey, M. Dolci and P. Zijlstra, *ACS Phys. Chem. Au*, 2023, **3**, 143–156.

129. H. Fu, X. Zhu, P. Li, M. Li, L. Yang, C. Jia and X. Guo, *J. Mater. Chem. C*, 2022, **10**, 2375–2389.

130. Y. Lv, J. Lin, K. Song, X. Song, H. Zang, Y. Zang and D. Zhu, *Sci. Adv.*, 2021, **7**, 3095.

131. D. Y. Zubarev, B. B. Averkiev, H. J. Zhai, L. S. Wang and A. I. Boldyrev, *Phys. Chem. Chem. Phys.*, 2007, **10**, 257–267.

132. X. Xie, P. Li, Y. Xu, L. Zhou, Y. Yan, L. Xie, C. Jia and X. Guo, *ACS Nano*, 2022, **16**, 3476–3505.

133. D. Xiang, H. Jeong, T. Lee and D. Mayer, *Adv. Mater.*, 2013, **25**, 4845–4867.

134. B. Xu and N. J. Tao, *Science*, 2003, **301**, 1221–1223.

135. Y. Zhu, Y. Zhou, L. Ren, J. Ye, H. Wang, X. Liu, R. Huang, H. Liu, J. Liu, J. Shi, P. Gao and W. Hong, *Angew. Chem. Int. Ed.*, 2023, **62**, e202302693.

136. A. Goetzberger, J. Luther and G. Willeke, *Sol. Energy Mater. Sol. Cells*, 2002, **74**, 1–11.

137. A. S. Al-Ezzi and M. N. M. Ansari, *Appl. Syst. Innov.*, 2022, **5**, 67.

138. D. J. Lipomi, *Joule*, 2018, **2**, 195–198.

139. Y. Ji, L. Xu, X. Hao and K. Gao, *Sol. RRL*, 2020, **4**, 2000130.

View Article Online
DOI: 10.1039/D5NR05504K

140. J. Wang, J. Li, Y. Zhou, C. Yu, Y. Hua, Y. Yu, R. Li, X. Lin, R. Chen, H. Wu, H. Xia and H. L. Wang, *J. Am. Chem. Soc.*, 2021, **143**, 7759–7768.

141. J.-P. Correa-Baena, M. Saliba, T. Buonassisi, M. Grätzel, A. Abate, W. Tress and A. Hagfeldt, *Science*, 2017, **358**, 739–744.

142. Y. Yang, S. Chen, Z. Dai, H. Wei, S. Wan, Y. Chen, J. Sun, Z. Liu, L. Ding, H. Xia, R. Chen and H. Wang, *Angew. Chem. Int. Ed.*, 2025, **64**, e202420262.

143. Z. Lu, Y. Cai, Y. Wei, Q. Lin, J. Chen, X. He, S. Li, W. Wu and H. Xia, *Polym. Chem.*, 2018, **9**, 2092–2100.

144. C. Yang, G. Lin, C. Zhu, X. Pang, Y. Zhang, X. Wang, X. Li, B. Wang, H. Xia and G. Liu, *J. Mater. Chem. B*, 2018, **6**, 2528–2535.

145. H. Zhang, H. Zhao, K. Zhuo, Y. Hua, J. Chen, X. He, W. Weng and H. Xia, *Polym. Chem.*, 2019, **10**, 386–394.

146. N. Lu, Z. Deng, J. Gao, C. Liang, H. Xia and P. Zhang, *Nat. Commun.*, 2022, **13**, 1–11.

147. H. Zhang, H. Zhao, K. Zhuo, Y. Hua, J. Chen, X. He, W. Weng and H. Xia, *Polym. Chem.*, 2019, **10**, 386–394.

148. B. Xu, W. Mao, C. Wu, J. Li, Z. Lu, M. Luo, L. L. Liu, L. Mao, D. Chen and H. Xia, *Chin. J. Chem.*, 2022, **40**, 1777–1784.

149. B. Xu, W. Mao, Z. Lu, Y. Cai, D. Chen and H. Xia, *Nat. Commun.*, 2024, **15**, 1–8.

150. X. Lai, S. Chen, X. Gu, H. Lai, Y. Wang, Y. Zhu, H. Wang, J. Qu, A. K. K. Kyaw, H. Xia and F. He, *Nat. Commun.*, 2023, **14**, 1–11.

View Article Online
DOI: 10.1039/D5NR05504K

Data sharing not applicable to this article as no datasets were generated or analyzed during the current study.